Electronic Supplementary Information for

Synthesis, Characterization and Luminescent Properties of Copper(I) Halide Complexes Containing Dimethylthiophene Bidentate Phosphine Ligand

Qiong Wei, Hong-Ting Chen, Li Liu*, Xin-Xin Zhong*, Lei Wang*, Fa-Bao Li, Hengjiang Cong*, Wai-Yeung Wong*, Khalid A. Alamry, Hai-Mei Qin

Contents

Experimental Details

1. NMR Experiments

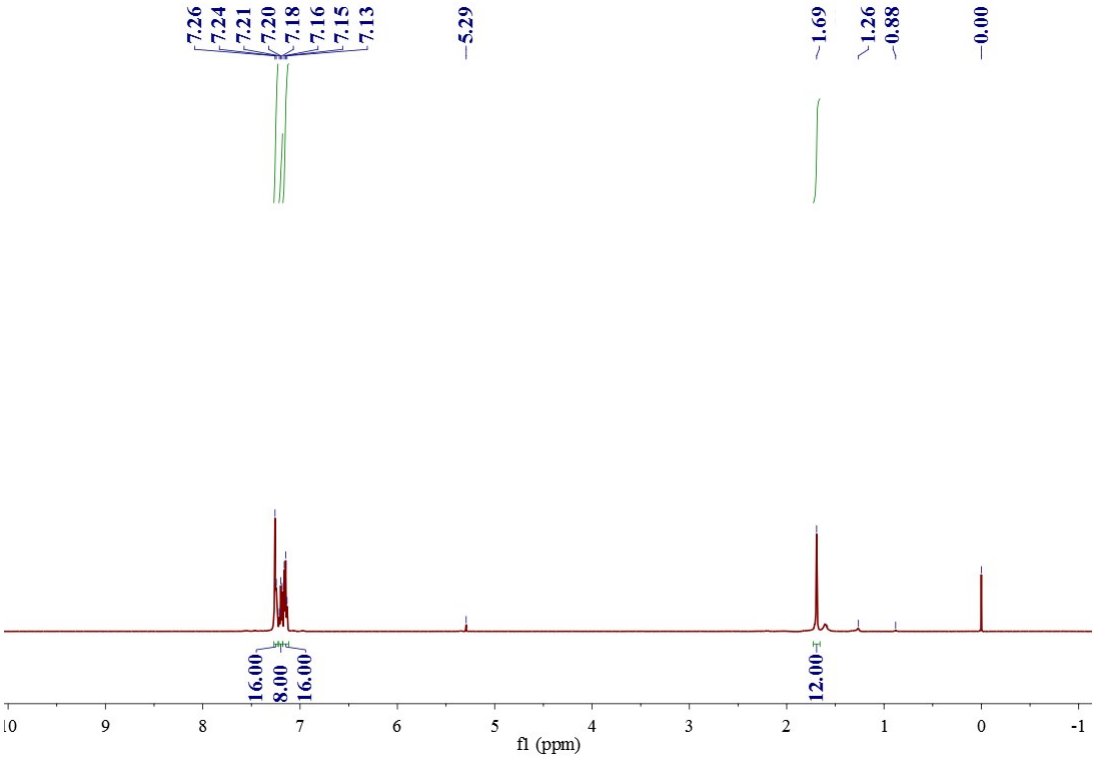

Fig. S1. ^{1}H NMR spectrum of **1** in $CDCl_3$.

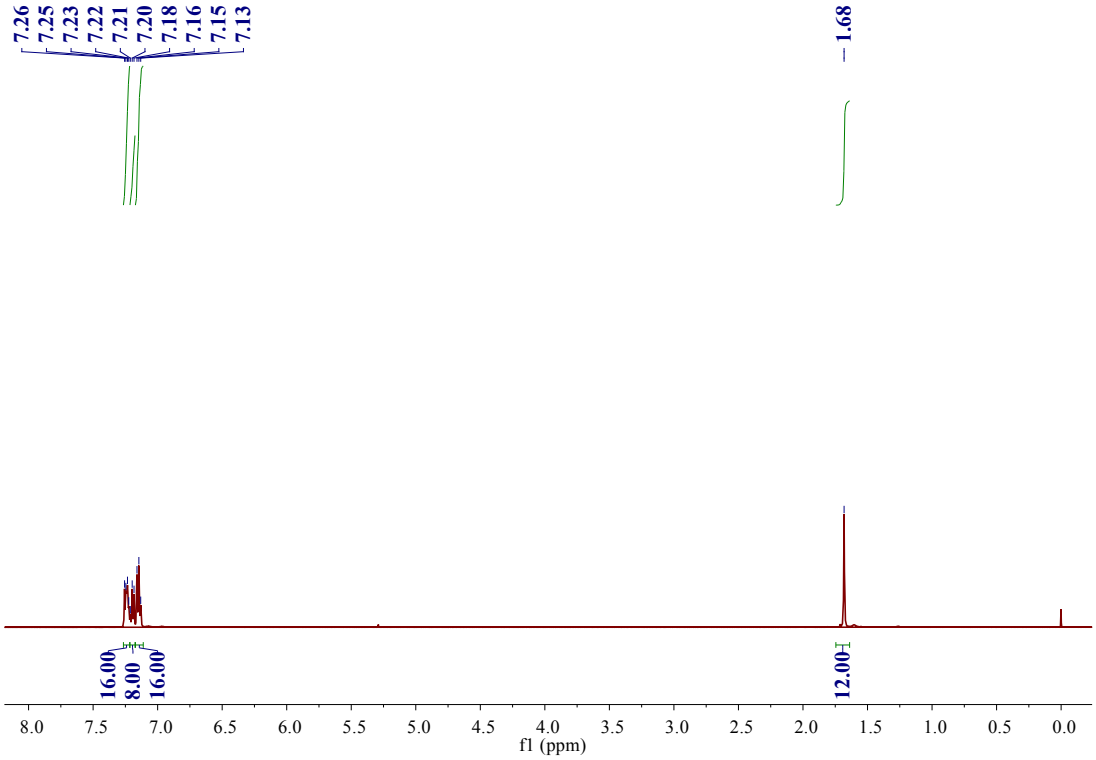

Fig. S2. ^{1}H NMR spectrum of **2** in $CDCl_3$.

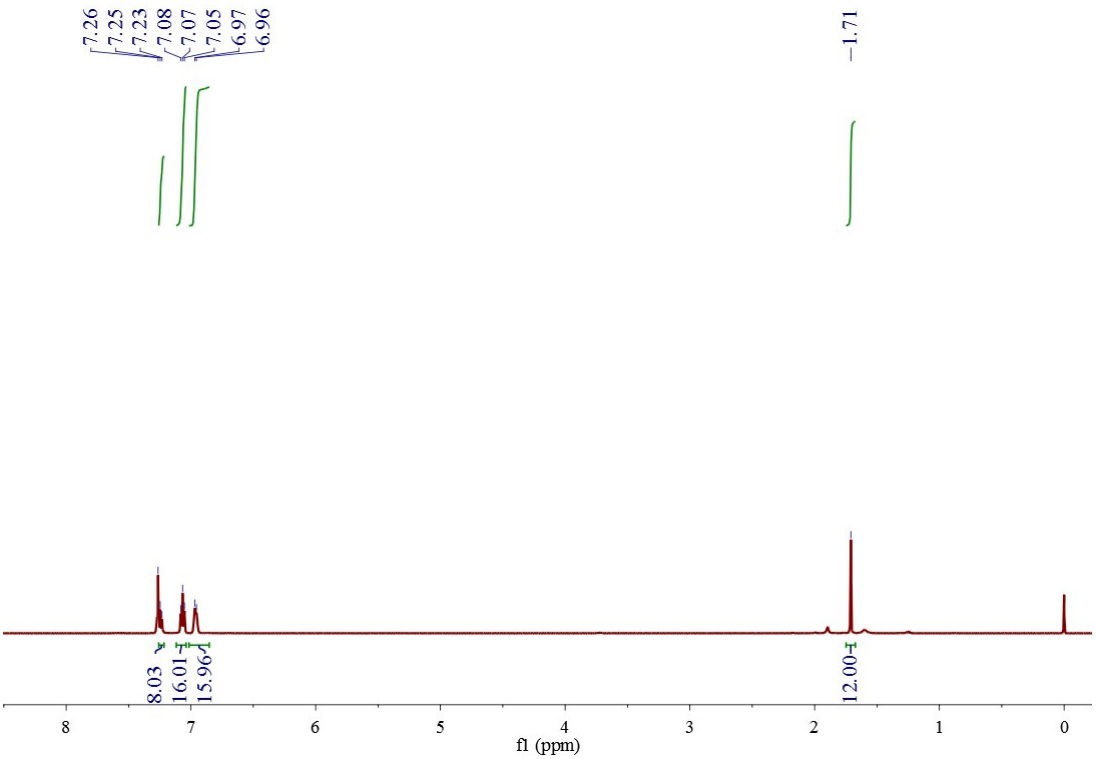

Fig. S3. ^{1}H NMR spectrum of **3** in $CDCl_3$.

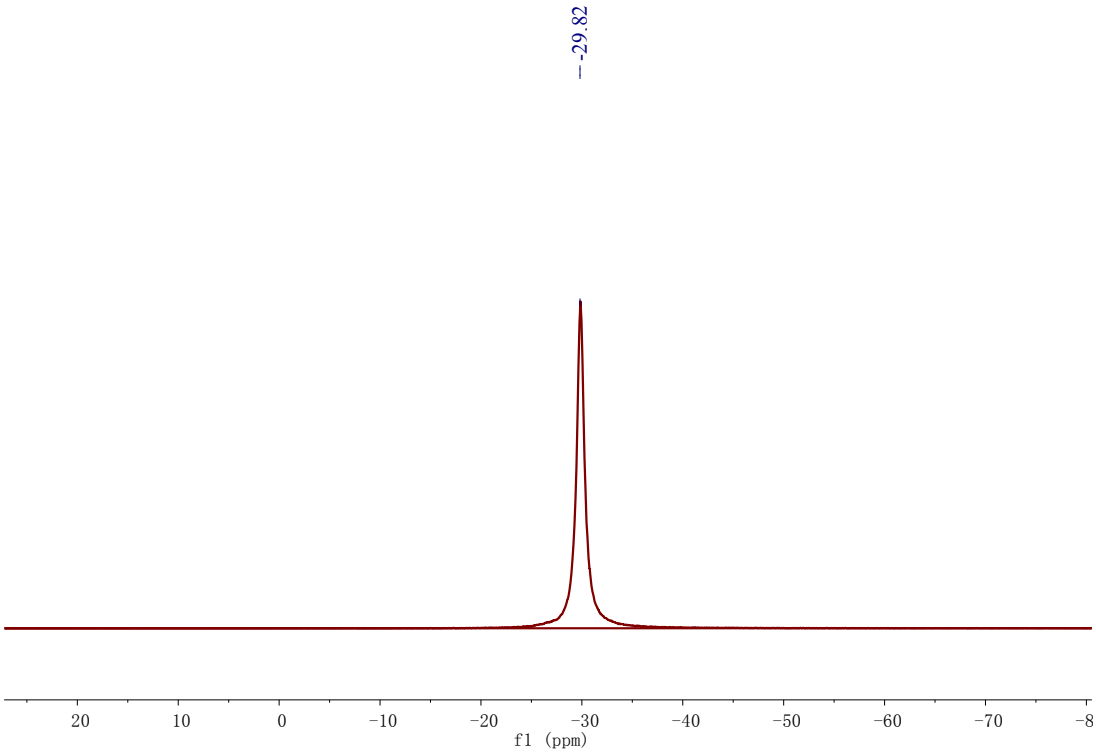

Fig. S4. ^{31}P NMR spectrum of **1** in $CDCl_3$.

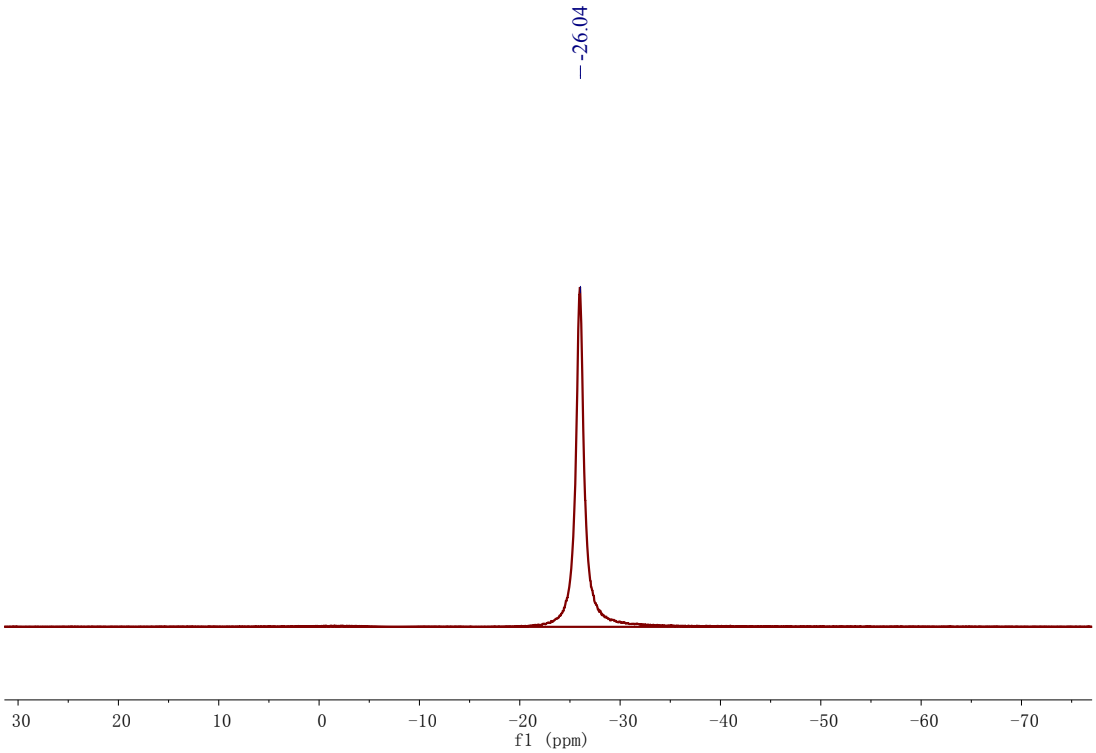

Fig. S5. ^{31}P NMR spectrum of **2** in $CDCl_3$.

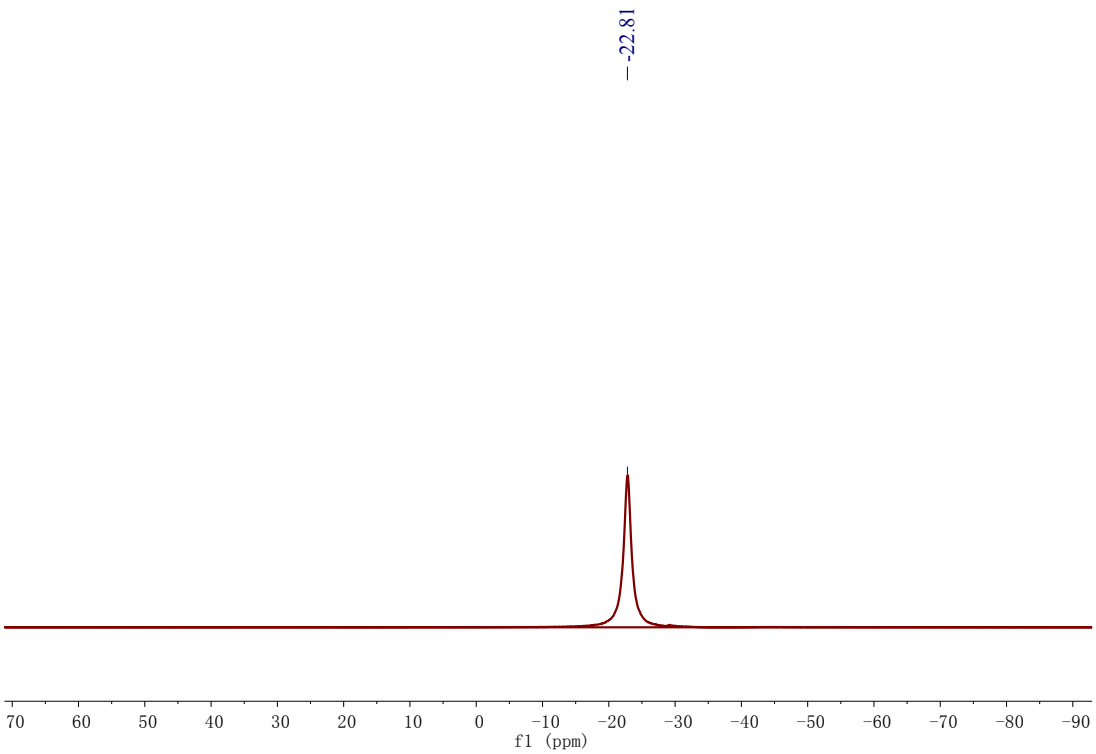

Fig. S6. ^{31}P NMR spectrum of **3** in $CDCl_3$.

2. MS spectra

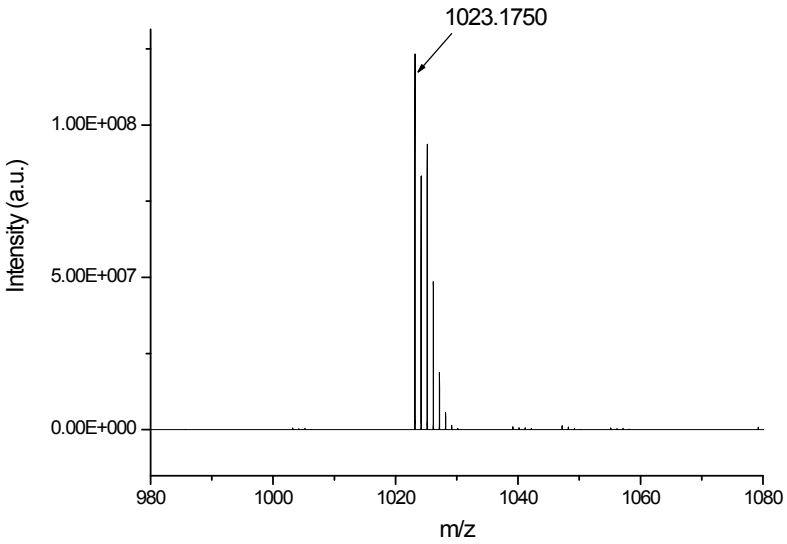

Fig. S7 MS spectrum of **1**.

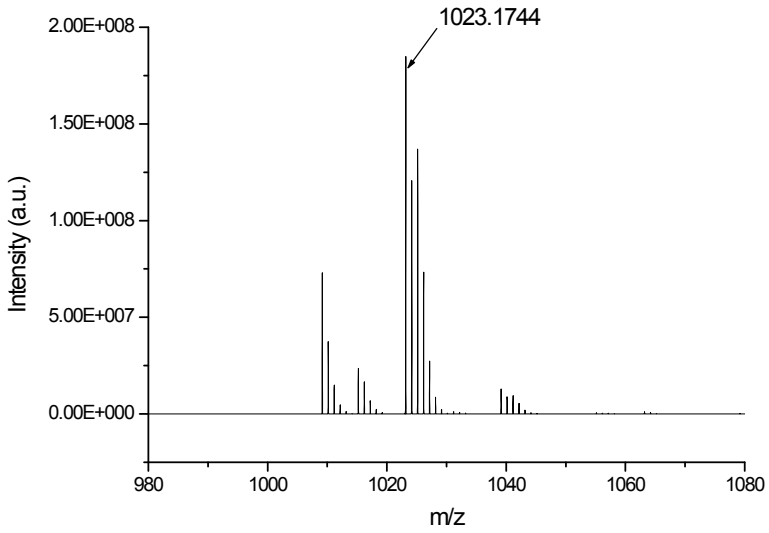

Fig. S8 MS spectrum of **2**.

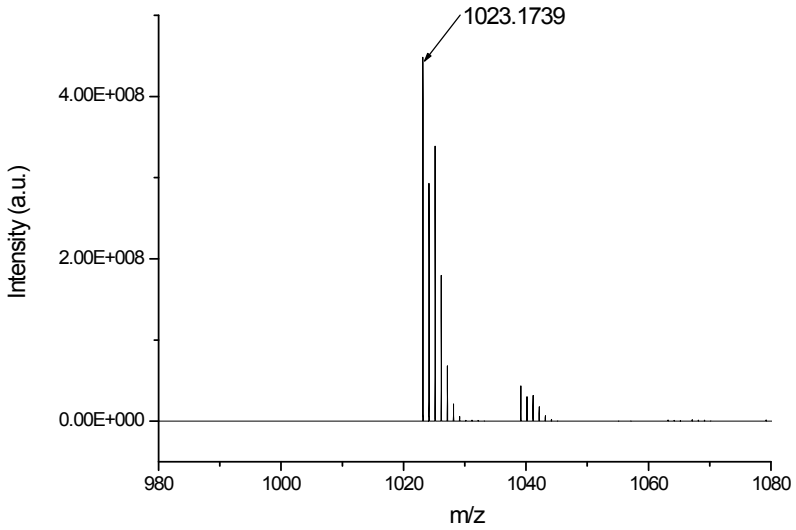

Fig. S9 MS spectrum of **3**.

3. Molecular structures

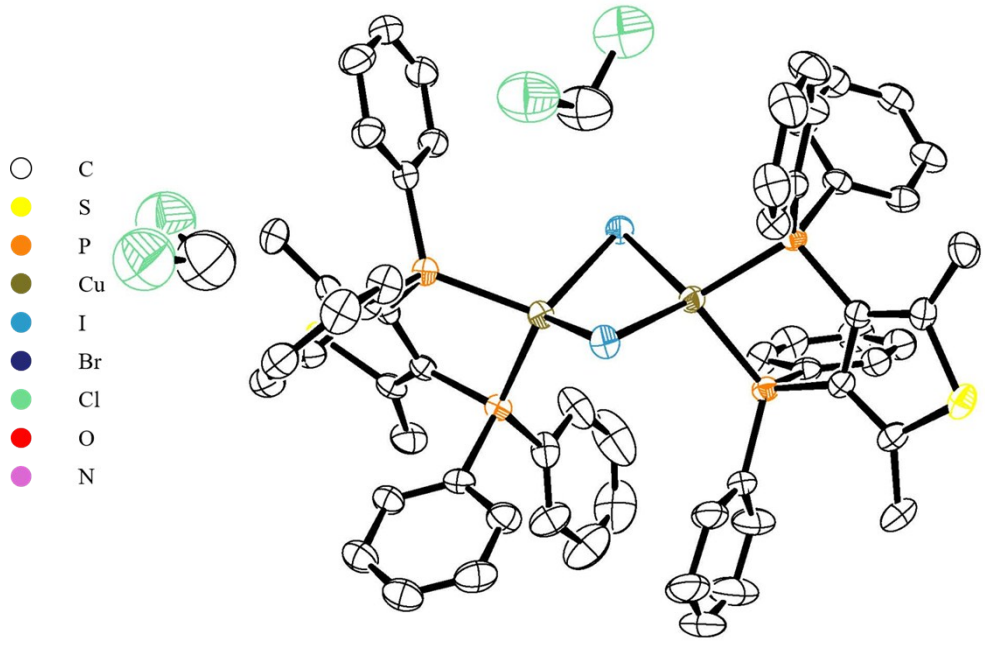

1

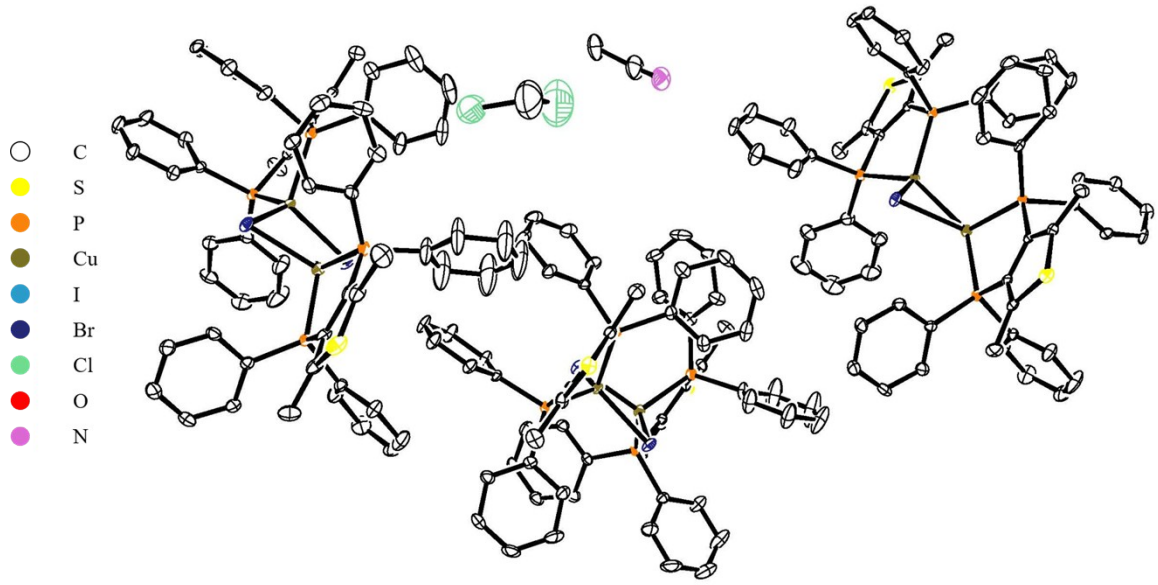

2

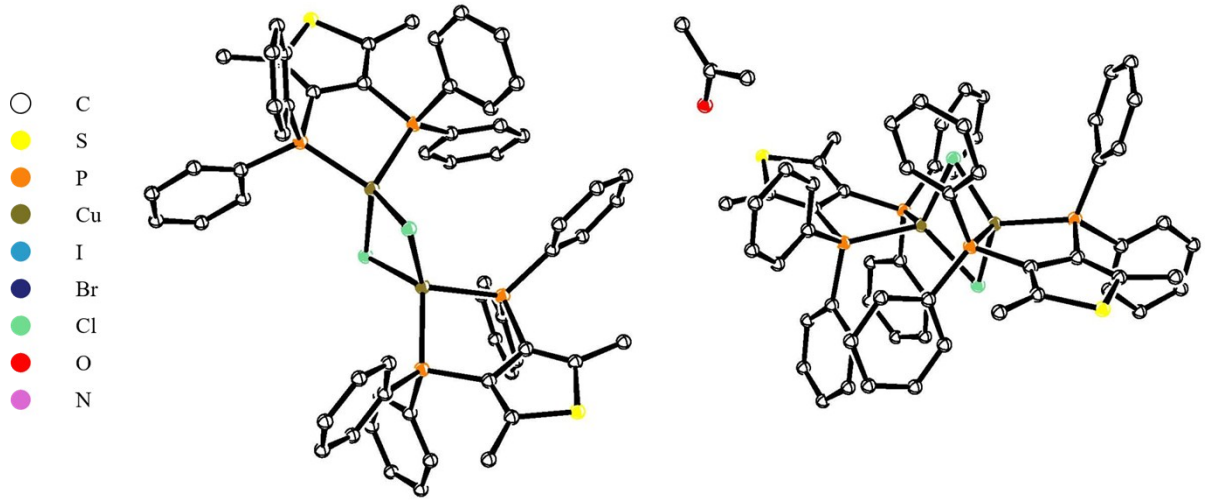

3

Fig. S10. ORTEP diagrams of complexes **1–3**. H atoms were omitted for clarity.

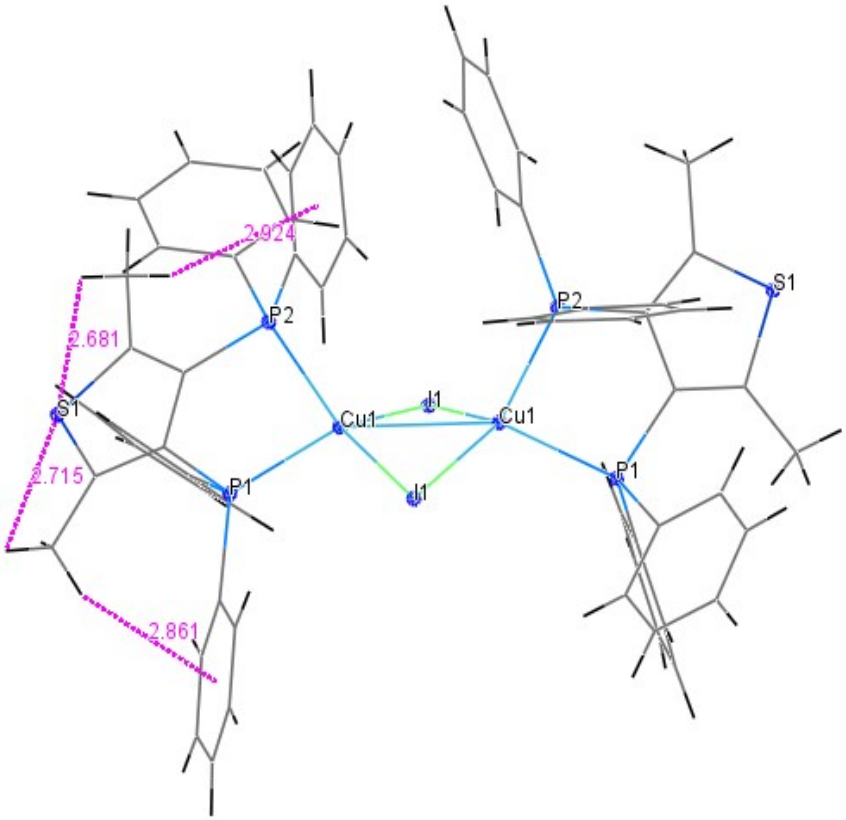

Fig. S11. Intramolecular S···C–H and C–H···π (phenyl) interactions in **1**.

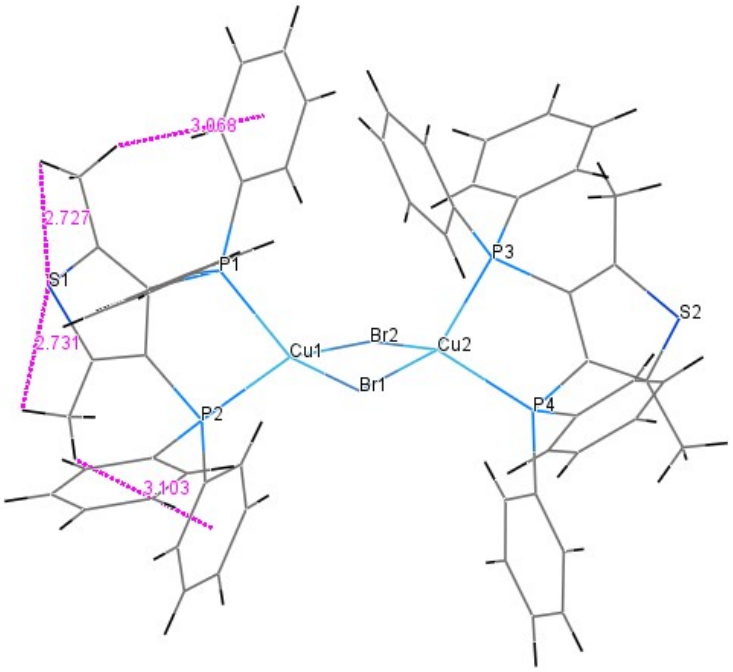

Fig. S12. Intramolecular S···C–H and C–H···π (phenyl) interactions in **2**.

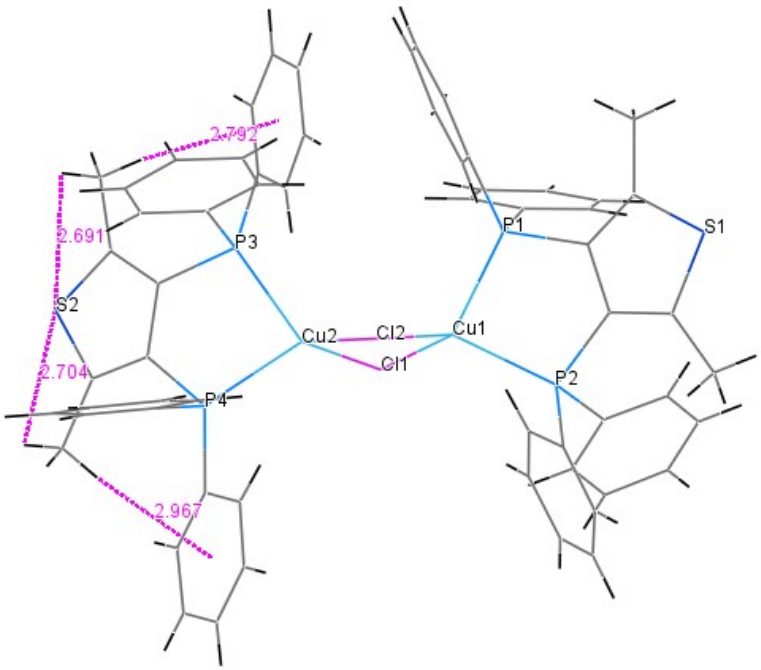

Fig. S13. Intramolecular S···C–H and C–H···π (phenyl) interactions in **3**.

.

2. Photophysical properties

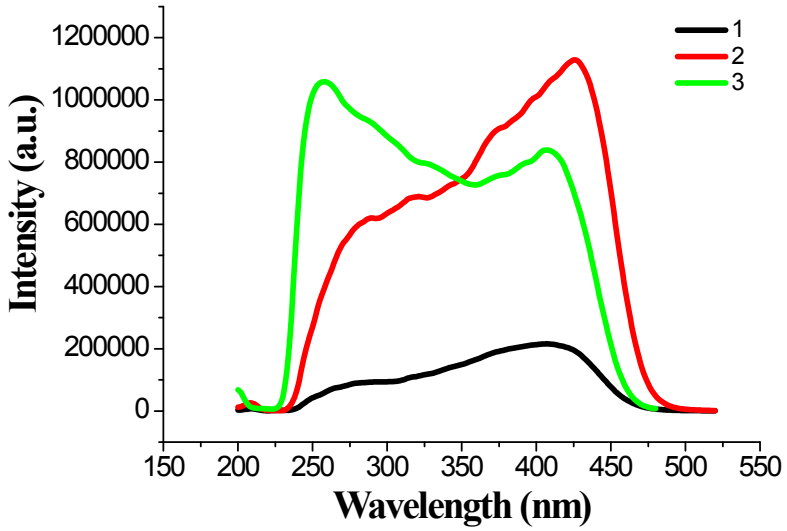

Fig. S14. Excitation spectra of **1-3** in the solid state (powders).

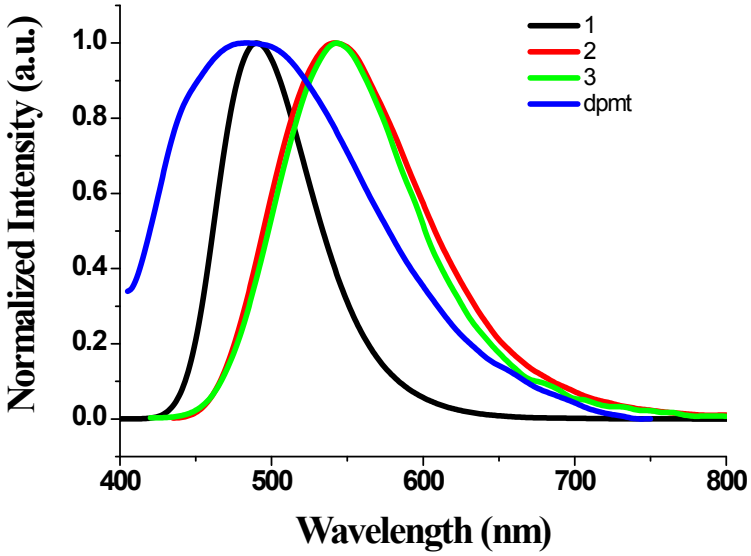

Fig. S15. PL spectra of ligand dpmt compared with complexes **1-3** in the solid state (powders) at 293 K.

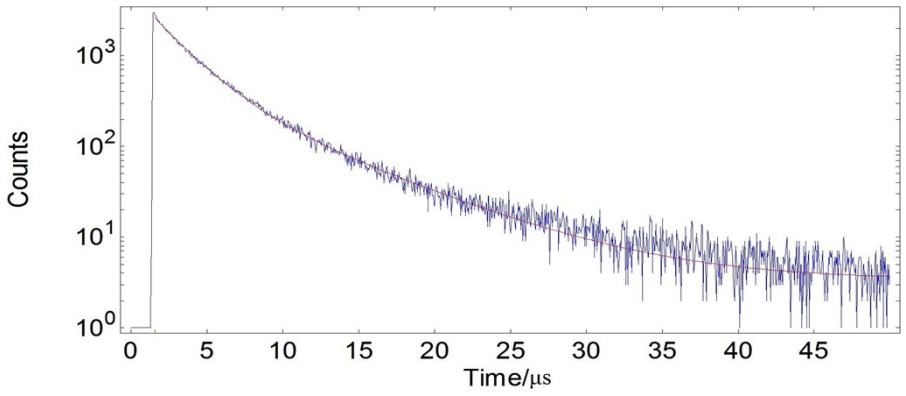

Fit = A + B1.exp(-t/T1) + B2.exp(-t/T2)

	Value	Std Dev		Value	Std Dev	Rel %
T1	2.185E-6	2.925E-8	B1	2.185E+3	2.089E+1	60.09
T2	6.519E-6	1.209E-7	B2	4.866E+2	2.253E+1	39.91
	Chisq	1.304E+0		A	3.391E+0	

Fig. S16. Time profiles of luminescence decay and exponential fit spectrum of **1** at r.t.

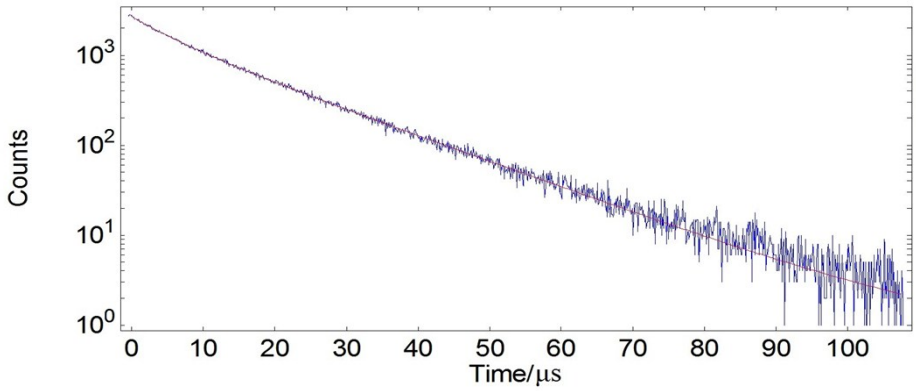

Fit = A + B1.exp(-t/T1) + B2.exp(-t/T2)

	Value	Std Dev		Value	Std Dev	Rel %
T1	5.736E-6	2.498E-7	B1	9.235E+2	3.796E+1	16.38
T2	1.515E-5	1.282E-7	B2	1.786E+3	4.181E+1	83.62
	Chisq	1.047E+0		A	7.530E-1	

Fig. S17. Time profiles of luminescence decay and exponential fit spectrum of **2** at r.t.

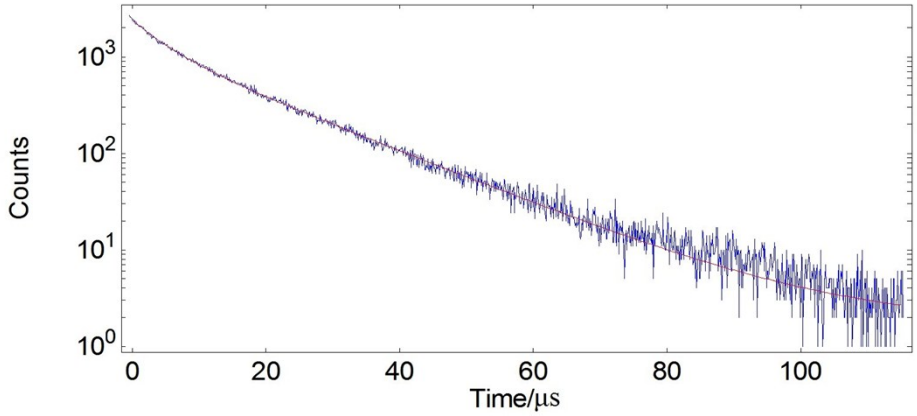

Fit = A + B1.exp(-t/T1) + B2.exp(-t/T2)

	Value	Std Dev		Value	Std Dev	Rel %
T1	4.677E-6	1.331E-7	B1	1.092E+3	2.037E+1	19.65
T2	1.578E-5	1.096E-7	B2	1.323E+3	2.128E+1	80.35
	Chisq	1.206E+0		A	1.781E+0	

Fig. S18. Time profiles of luminescence decay and exponential fit spectrum of **3** at r.t.

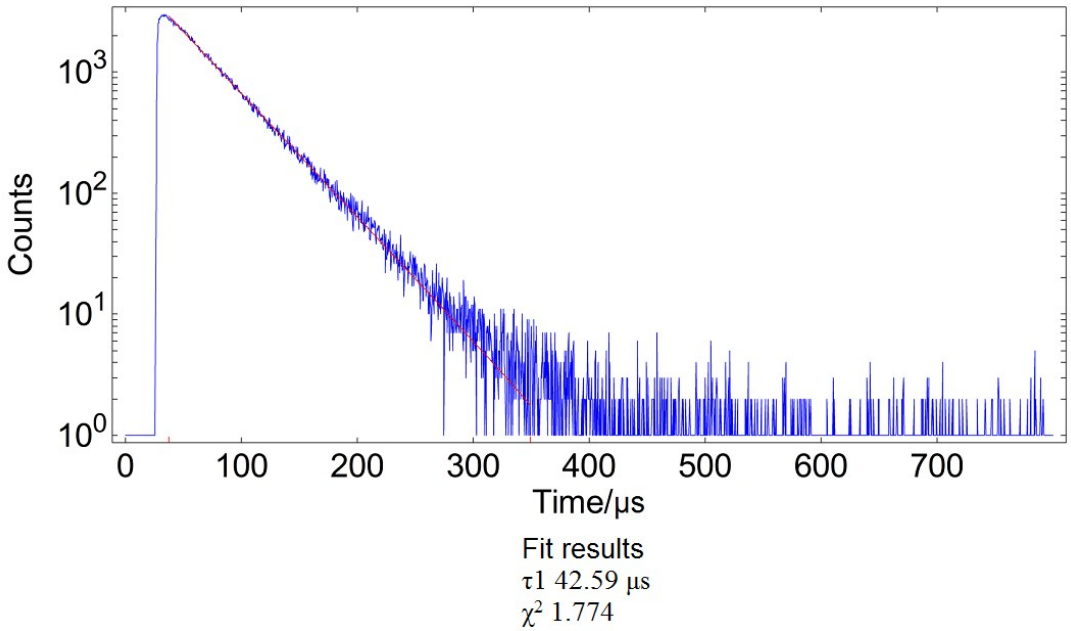

Fig. S19. Time profiles of luminescence decay and exponential fit spectrum of **1** at 77 K.

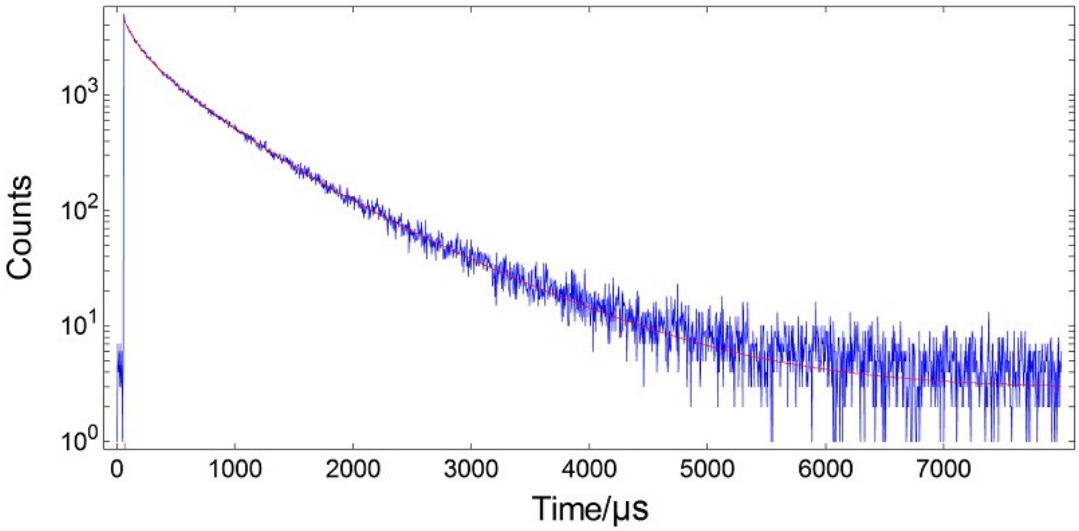

Fit = A + B1.exp(-t/T1) + B2.exp(-t/T2) + B3.exp(-t/T3)

	Value	Std Dev		Value	Std Dev	Rel %
T1	1.075E-4	4.928E-6	B1	1.610E+3	5.422E+1	9.84
T2	4.374E-4	1.540E-5	B2	2.027E+3	4.395E+1	50.40
T3	9.402E-4	2.283E-5	B3	7.442E+2	6.931E+1	39.77
	Chisq	1.280E+0		A	2.867E+0	

Fig. S20. Time profiles of luminescence decay and exponential fit spectrum of **2** at 77 K.

	Value	Std Dev		Value	Std Dev	Rel %
T1	6.168E-6	2.677E-7	B1	1.483E+3	4.466E+1	4.27
T2	7.124E-5	1.371E-6	B2	1.018E+3	1.337E+1	33.88
T3	3.197E-4	3.253E-6	B3	4.143E+2	7.584E+0	61.85
	Chisq	1.411E+0		A	2.806E+0	

Fig. S21. Time profiles of luminescence decay and exponential fit spectrum of **3** at 77 K.

4. Computational details

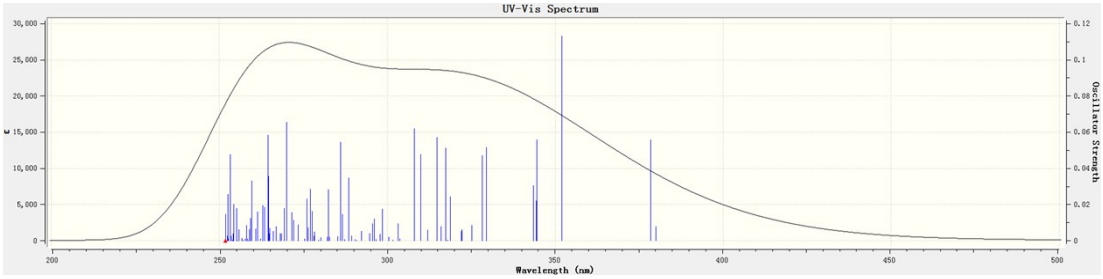

Fig. S22. The absorption spectrum of complex **1** in CH_2Cl_2.

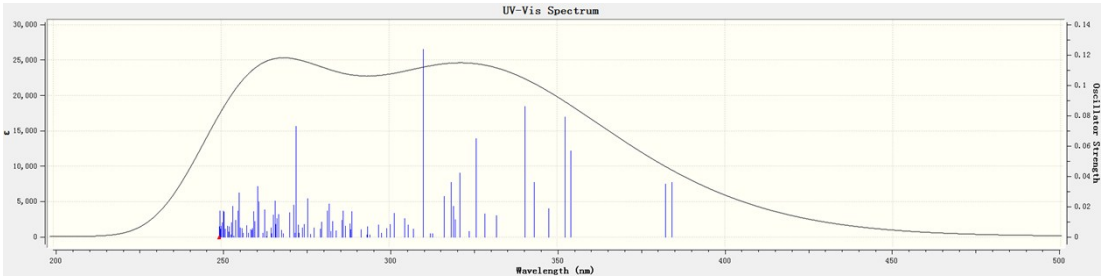

Fig. S23. The absorption spectrum of complex **2** in CH_2Cl_2.

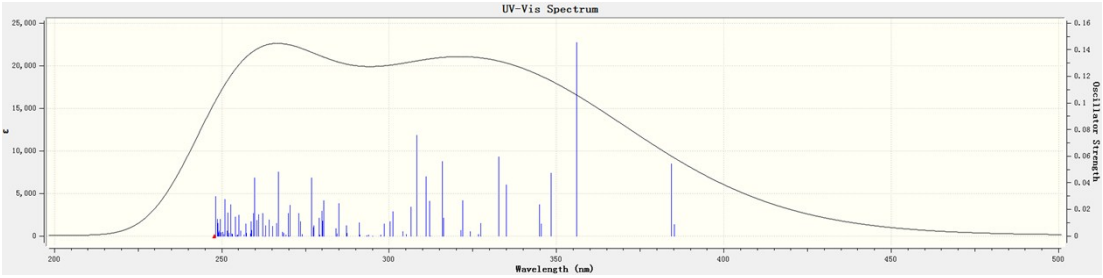

Fig. S24. The absorption spectrum of complex **3** in CH_2Cl_2.

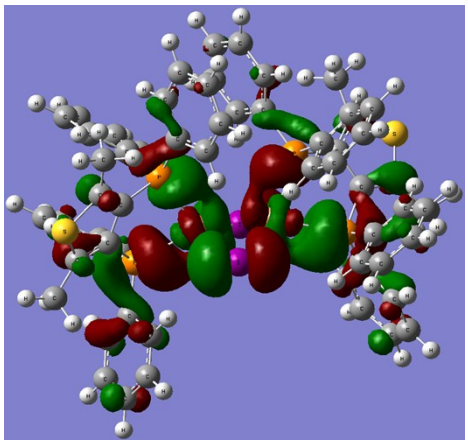

HOMO

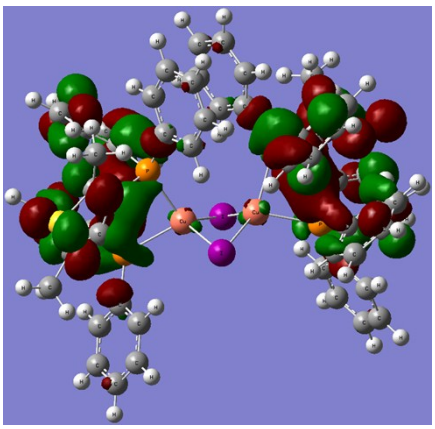

LUMO

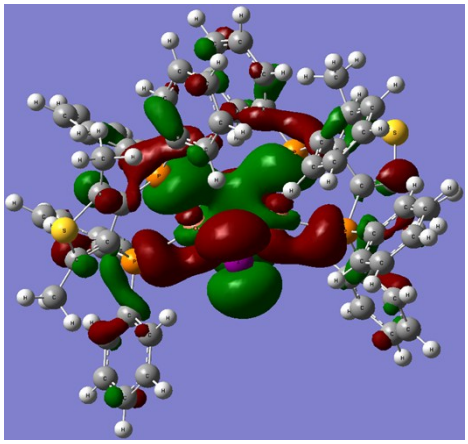

HOMO−1

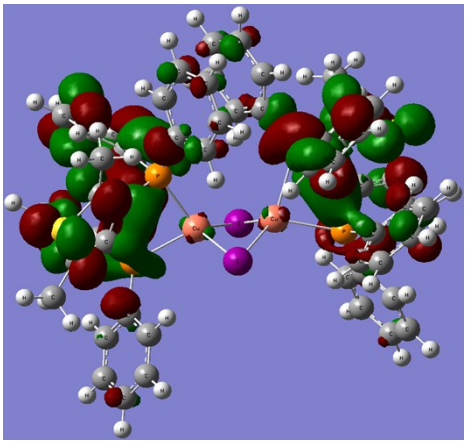

LUMO+1

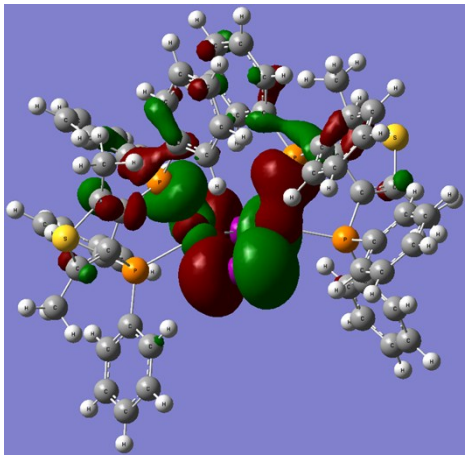

HOMO−2

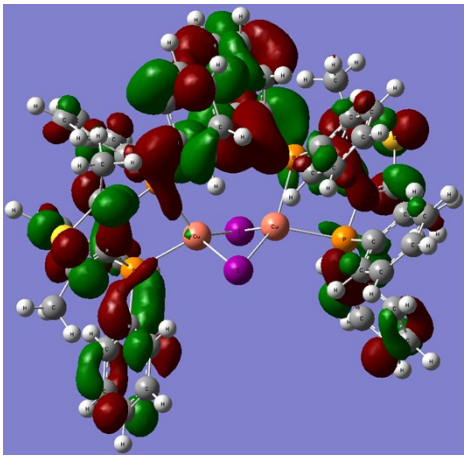

LUMO+2

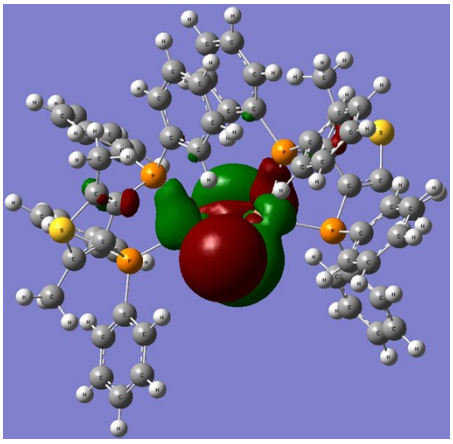

HOMO−3

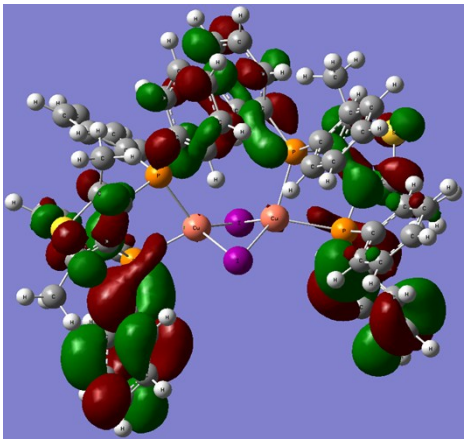

LUMO+3

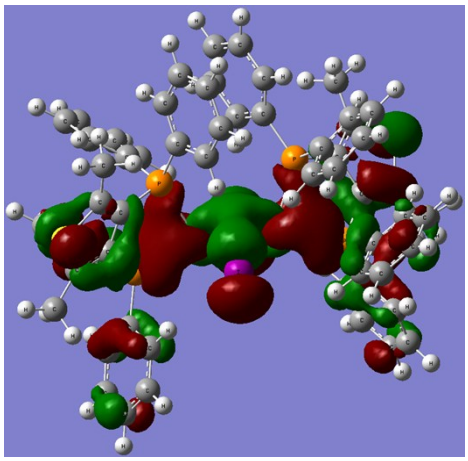

HOMO–4

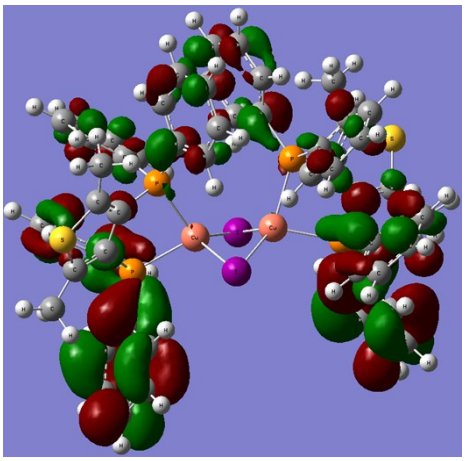

LUMO+4

1

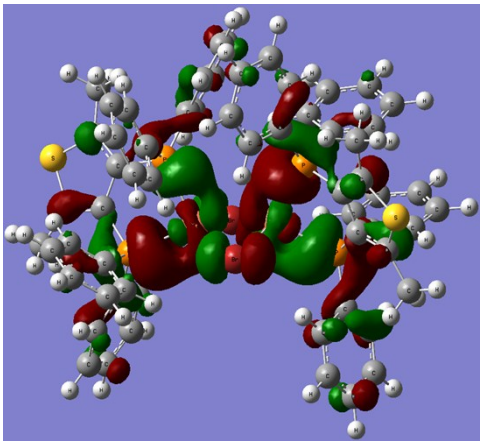

HOMO

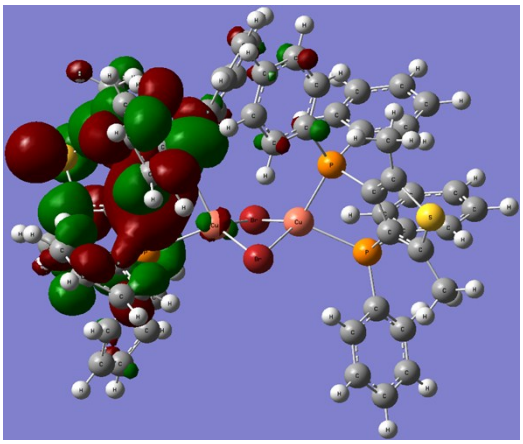

LUMO

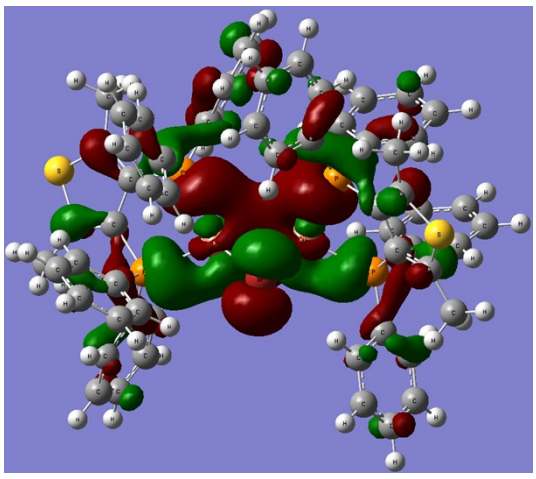

HOMO–1

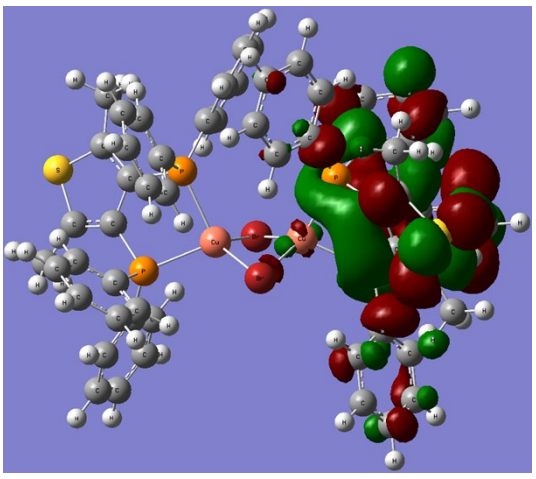

LUMO+1

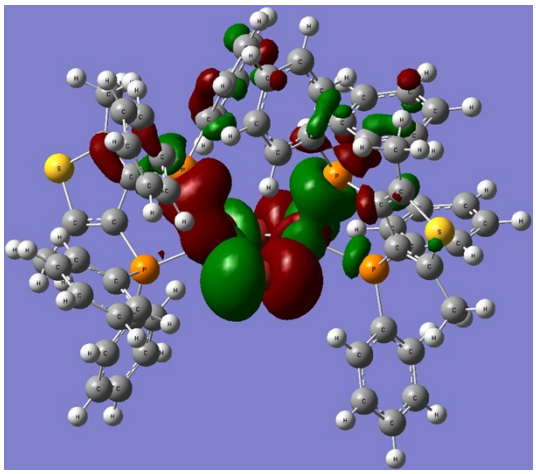

HOMO−2

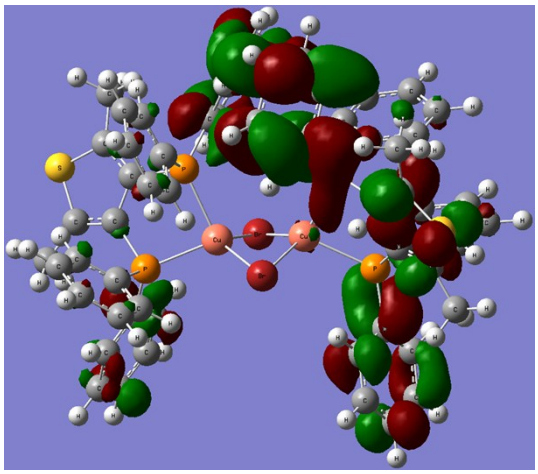

LUMO+2

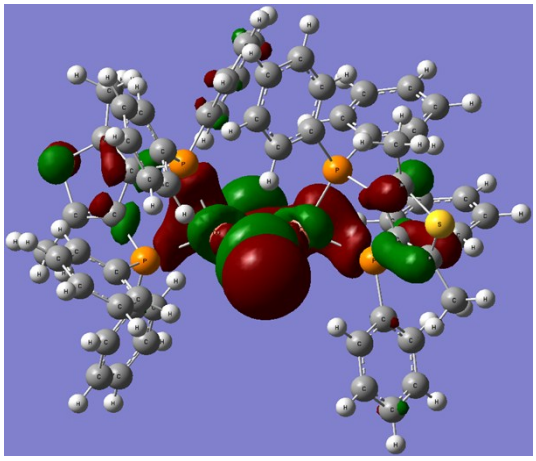

HOMO−3

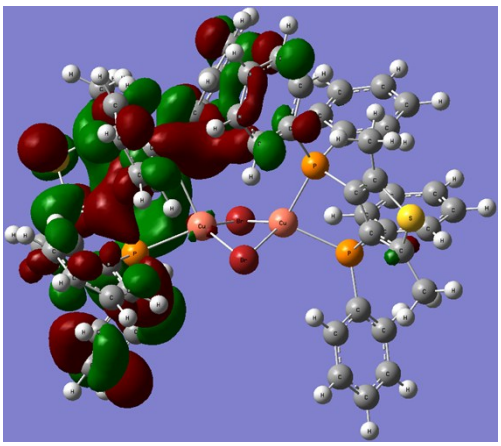

LUMO+3

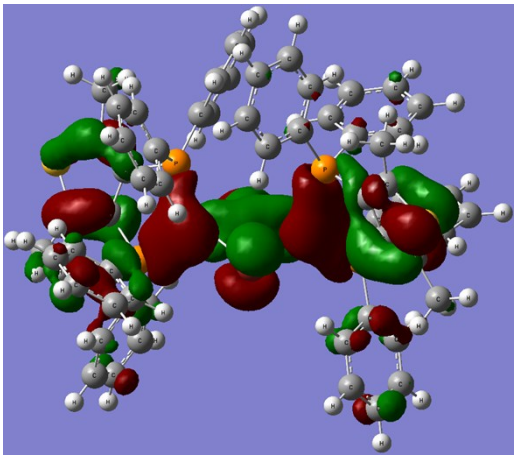

HOMO−4

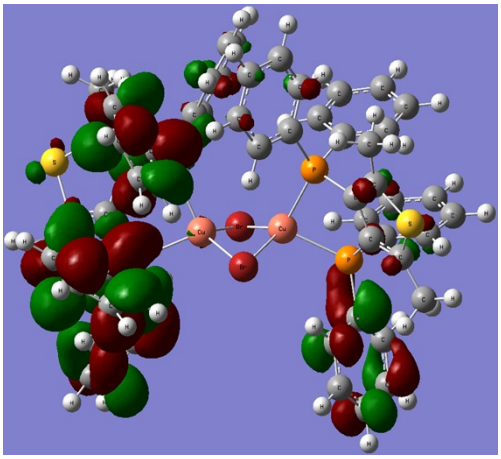

LUMO+4

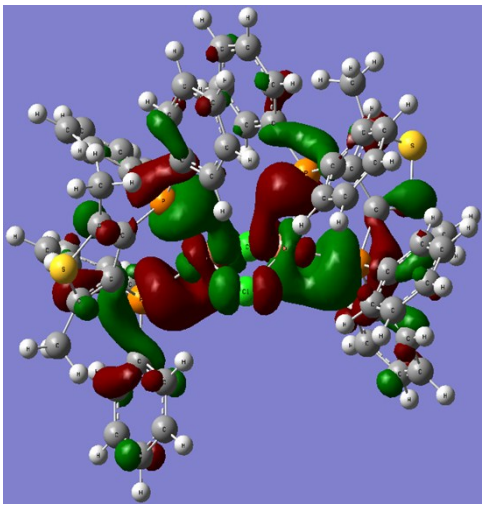

HOMO

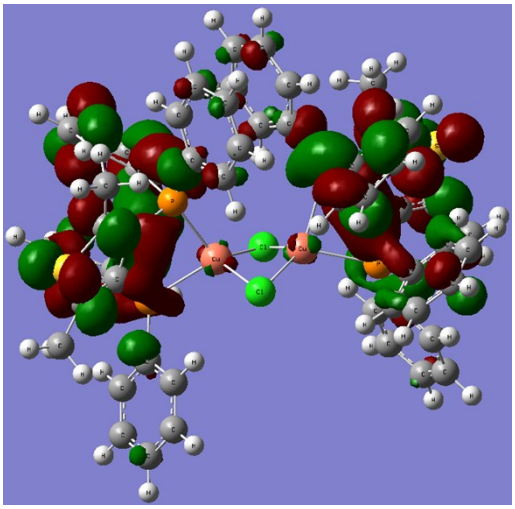

LUMO

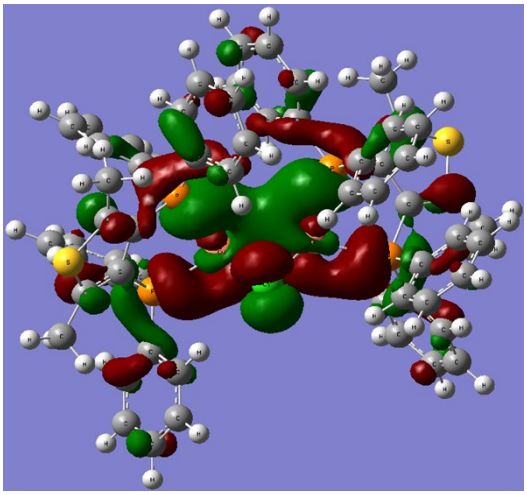

HOMO−1

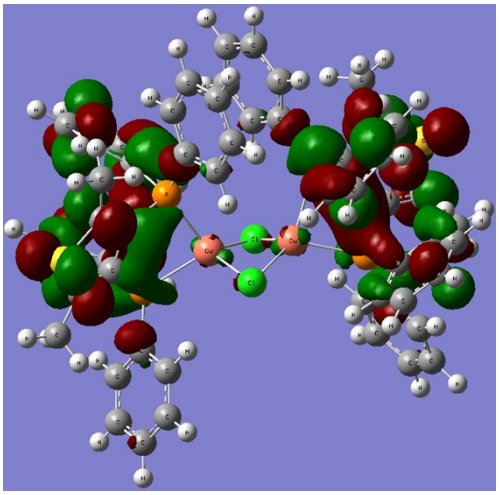

LUMO+1

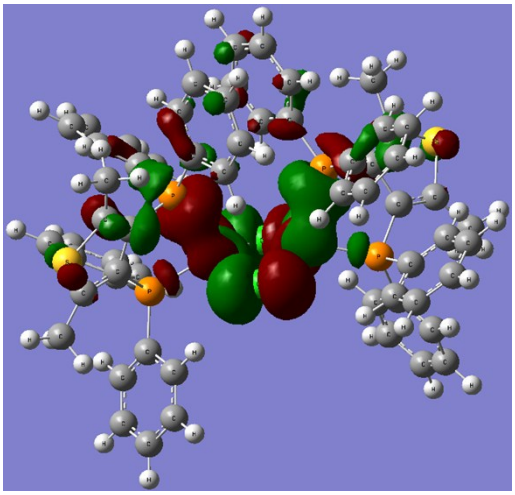

HOMO−2

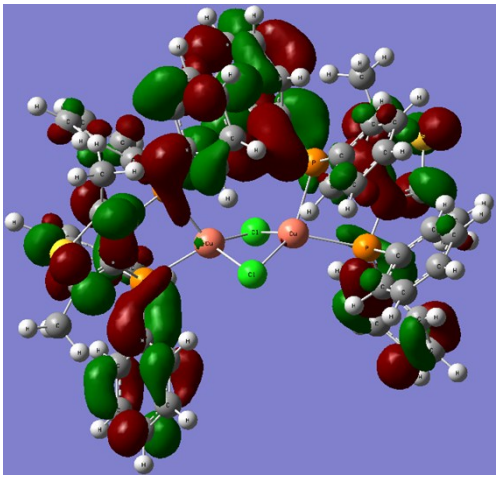

LUMO+2

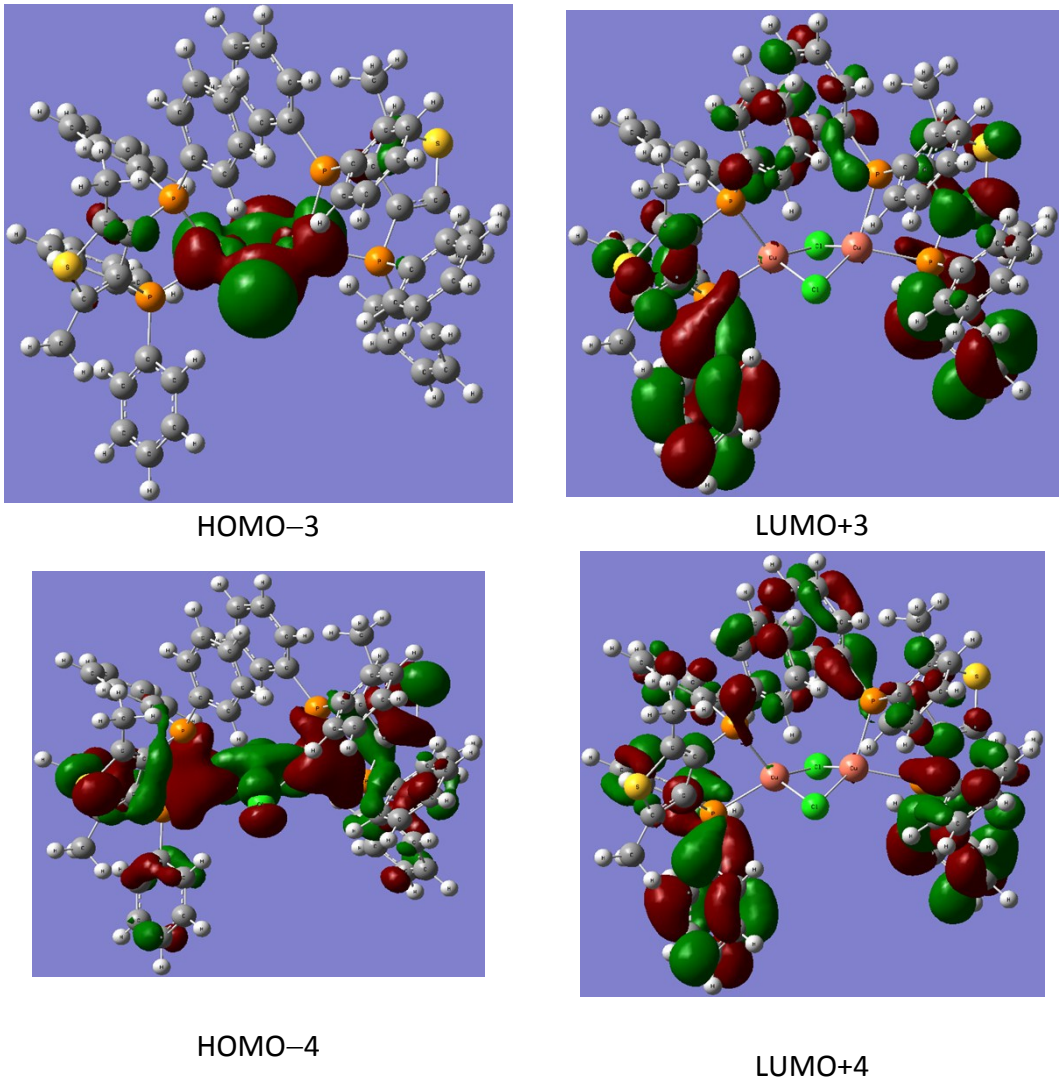

Fig. S25. Contour plots of frontier molecular orbitals of complexes **1-3** in CH_2Cl_2.

Table S1. Computed excitation states for complex **1** in CH_2Cl_2.

State	λ(nm)/*E*(eV)	Configurations	*f*
1	352.9 (3.51)	H-1→L+1 (42); H→L(56)	0.0042
5	311.9 (3.97)	H-1→L+3 (28); H→L+2 (67)	0.0689
6	310.4 (3.99)	H-1→L+2 (63); H→L+3 (31)	0.4402
8	302.7 (4.10)	H-2→L+1 (82); H-1→L (8); H→L+5 (3)	0.0844
9	298.9 (4.15)	H-2→L+1 (3); H-1→L+3 (9); H-1→L+4 (40); H→L+2 (3); H→L+5 (39)	0.1005
11	297.9 (4.16)	H-1→L+3 (16); H-1→L+4 (8); H-1→L+7 (16); H→L+2 (11); H→L+6 (43)	0.0710
14	293.3 (4.23)	H-3→L (8); H-1→L+2 (11); H-1→L+5 (3); H-1→L+6 (15); H-1→L+8 (6); H→L+3 (29); H→L+7 (23)	0.0542
16	290.0 (4.28)	H-3→L+1 (93); H→L+8 (2)	0.0827

42	265.6 (4.67)	H-4→L (65); H-2→L+5 (15); H-2→L+6 (3)	0.0700
52	258.5 (4.80)	H-8→L (35); H-7→L+1 (11); H-6→L+1 (29); H-2→L+9 (9); H→L+14 (4)	0.0549
53	258.4 (4.80)	H-8→L+1 (12); H-7→L (5); H-6→L (11); H-2→L+8 (52); H-2→L+10 (2); H-1→L+13 (4); H-1→L+19 (2); H→L+18 (4)	0.0674
57	256.5 (4.83)	H-3→L+5 (37); H-2→L+8 (4); H-2→L+10 (5); H-1→L+14 (8); H-1→L+19 (6); H→L+15 (11); H→L+17 (2); H→L+18 (18)	0.0604
59	255.1 (4.86)	H-7→L (49); H-6→L (20); H-4→L+2 (2); H-3→L+5 (6); H-3→L+6 (9); H-2→L+10 (8)	0.0874

Table S2. Computed excitation states for complex **2** in CH_2Cl_2.

State	λ(nm)/*E*(eV)	Configurations	*f*
1	355.7 (3.49)	H-1→L (23); H-1→L+1 (4); H→L (69); H→L+1 (2)	0.0057
3	317.8 (3.90)	H-1→L+2 (47); H-1→L+3 (3); H→L+2 (37); H→L+3 (10)	0.1633
5	314.7 (3.94)	H-1→L (13); H-1→L+1 (7); H-1→L+3 (17); H→L (7); H→L+2 (15); H→L+3 (36)	0.2419
9	303.1 (4.09)	H-2→L+1 (6); H-1→L+5 (37); H→L+5 (47)	0.2326
10	301.8 (4.11)	H-2→L+1 (37); H-1→L+5 (4); H-1→L+6 (12); H→L+5 (2); H→L+6 (37)	0.0815
18	284.9 (4.35)	H-1→L+4 (8); H-1→L+9 (3); H-1→L+11 (17); H→L+4 (7); H→L+10 (43); H→L+11 (11)	0.0555
24	278.5 (4.45)	H-3→L+1 (61); H-2→L+2 (3); H-2→L+3 (3); H-1→L+12 (4); H-1→L+13 (8); H→L+12 (2); H→L+13 (11)	0.0518
48	258.6 (4.80)	H-7→L (16); H-6→L (63); H-6→L+1 (5); H-2→L+8 (6)	0.0610
49	257.0 (4.82)	H-2→L+9 (5); H-1→L+14 (4); H-1→L+17 (4); H-1→L+18 (16); H→L+14 (6); H→L+17 (4); H→L+18 (42)	0.0664
60	251.8 (4.92)	H-7→L+1 (32); H-6→L+1 (16); H-5→L+1 (4); H-2→L+9 (2); H-1→L+14 (4); H-1→L+19 (13); H→L+19 (13)	0.0688
70	243.5 (5.09)	H-8→L (77); H-3→L+7 (2); H-2→L+15 (5)	0.0921

Table S3. Computed excitation states for complex **3** in CH_2Cl_2.

State	λ(nm)/*E*(eV)	Configurations	*f*
1	355.5 (3.49)	H-1→L+1 (40); H→L(58)	0.0004
6	313.5 (3.95)	H-1→L+2 (54); H→L+3 (42)	0.4579
8	302.0 (4.11)	H-1→L+3 (5); H-1→L+4 (42); H→L+5 (40); H→L+6 (6)	0.2023
9	300.3 (4.13)	H-1→L+3 (6); H-1→L+4 (5); H-1→L+7 (24); H→L+2 (6); H→L+5 (7); H→L+6 (49)	0.0866
10	300.1 (4.13)	H-2→L (2); H-1→L+2 (12); H-1→L+6 (44); H→L+3 (10); H→L+7 (29)	0.0669
16	290.2 (4.27)	H-4→L (2); H-2→L+1 (56); H-1→L+9 (14); H→L+8 (18)	0.0694
26	274.2 (4.52)	H-8→L (3); H-3→L+1 (91)	0.0653
39	260.1 (4.77)	H-5→L+1 (11); H-4→L (35); H-2→L+5 (18); H-2→L+6 (24)	0.0512

42	258.1 (4.80)	H-6→L+1 (9); H-5→L (22); H-4→L+1 (10); H-2→L+4 (53)	0.0698
50	253.7 (4.89)	H-1→L+14 (6); H-1→L+19 (22); H-1→L+21 (2); H→L+15 (7); H→L+18 (51); H→L+20 (3)	0.1117
68	242.1 (5.12)	H-8→L (67); H-7→L+1 (5); H-3→L+1 (4); H-3→L+6 (6); H-3→L+8 (2); H-2→L+12 (5)	0.0728

Table S4. Calculated emission wavelength (λ), oscillator strength (f) and main configuration of three complexes along with their experimental values (λ_{exp}).

	λ (nm)	f	Main configurations	$\lambda_{expt.}$ (nm)
1	473	0.0113	HOMO→LUMO (99%)	490
2	525	0.0053	HOMO→LUMO (99%)	542
3	499	0.0141	HOMO→LUMO (99%)	543